

## Fractal-like image statistics in visual art: similarity to natural scenes

CHRISTOPH REDIES<sup>1,\*</sup>, JENS HASENSTEIN<sup>2</sup> and JOACHIM DENZLER<sup>2</sup>

<sup>1</sup>*Institute of Anatomy I, School of Medicine, Friedrich Schiller University, D-07740 Jena, Germany*

<sup>2</sup>*Department of Computer Science, Friedrich Schiller University, D-07740 Jena, Germany*

Received 12 June 2006; accepted 19 February 2007

**Abstract**—Both natural scenes and visual art are often perceived as esthetically pleasing. It is therefore conceivable that the two types of visual stimuli share statistical properties. For example, natural scenes display a Fourier power spectrum that tends to fall with spatial frequency according to a power-law. This result indicates that natural scenes have fractal-like, scale-invariant properties. In the present study, we asked whether visual art displays similar statistical properties by measuring their Fourier power spectra. Our analysis was restricted to graphic art from the Western hemisphere. For comparison, we also analyzed images, which generally display relatively low or no esthetic quality (household and laboratory objects, parts of plants, and scientific illustrations). Graphic art, but not the other image categories, resembles natural scenes in showing fractal-like, scale-invariant statistics. This property is universal in our sample of graphic art; it is independent of cultural variables, such as century and country of origin, techniques used or subject matter. We speculate that both graphic art and natural scenes share statistical properties because visual art is adapted to the structure of the visual system which, in turn, is adapted to process optimally the image statistics of natural scenes.

*Keywords:* Fourier analysis; natural vision; graphic art; Western culture; fractal properties.

### 1. INTRODUCTION

The visual system of higher mammals is adapted to process optimally the information encoded in natural stimuli (Field, 1987; Parraga *et al.*, 2000; Simoncelli and Olshausen, 2001). For example, responses of visual neurons to natural scenes are highly decorrelated, allowing for efficient coding of visual information in a relatively low number of neurons ('sparse coding') (Hoyer and Hyvärinen, 2002; Olshausen and Field, 1996; Vinje and Gallant, 2000, 2002). Sparseness is a coding principle also in the other sensory systems and in the motor system of the brain (for review, see Hahnloser *et al.*, 2002; Lewicki, 2002; Olshausen and Field, 2004).

---

\*To whom correspondence should be addressed. E-mail: [redies@mti.uni-jena.de](mailto:redies@mti.uni-jena.de)

One characteristic feature of complex natural scenes is their scale invariance, that is, when zooming in and out of a natural scene, the statistical properties of the Fourier spectral components remain relatively constant. This fractal-like property is reflected in the empirical finding that the spectral power of natural scenes falls with spatial frequencies,  $f$ , according to a power law,  $1/f^p$ , with values of  $p$  near 2 (Burton and Moorhead, 1987; Field, 1987; Ruderman and Bialek, 1994; Simoncelli and Olshausen, 2001; Tolhurst *et al.*, 1992;).

In a search for universal features that characterize esthetic visual stimuli, we here consider that both natural scenes and visual art are often perceived as esthetically pleasing (for an introductory review, see Redies, 2007, in this issue). Consequently, it is conceivable that the two types of visual stimuli share statistical properties. We therefore asked whether the Fourier power spectra of visual art are similar to those of natural images.

We restrict our analysis to monochrome (grayscale) graphic art from Western cultures. Graphic art has the advantage that reproductions of high quality for different artists, centuries, techniques and cultures are readily accessible in art books. Artefacts introduced after the creation of the work, such as fading of color pigments and discoloring of varnish, can be excluded more readily than for colored oil paintings, watercolors, etc. Care was taken to include a wide variety of different artists, styles, techniques and subject matter in the analysis. Examples of art analyzed ranged from 15th century engravings to 20th century abstract drawings. The majority of graphic art analyzed in the present study was created by well-known artists and collected by prestigious museums. It seems reasonable to assume that these works of art were preserved over time mainly because of their esthetic value. Because we trusted the esthetic judgment of generations of art collectors and custodians, no attempt was made to confirm psychophysically the esthetic quality of the art included in the present study. Contemporary, non-esthetic art (see discussion in Redies, 2007) was not included in the analysis.

As controls, we analyzed three other types of images with generally low or no esthetic appeal (images of household or laboratory objects, of plants, and scientific illustrations). Images of household and laboratory objects were chosen because they depict objects whose appearance is determined mostly by their functionality rather than their esthetic value. In these images, the objects are generally positioned randomly or according to non-esthetic considerations. Images of plants or parts of plants were chosen because most of them, in contrast to natural scenes, do not show a fractal structure. For example, when magnifying a set of uniformly colored leaves, the statistical structure of the leaves is not repeated in the leaves themselves (with the exception of plants like ferns). Scientific illustrations were used as another example of drawings made by humans. Although scientific illustrations may have high esthetic appeal in exceptional cases (for example, the illustrations by Leonardo da Vinci), the purpose of most illustrations found in modern textbooks is to convey scientific information; their esthetic quality is only a minor determinant in their production in most cases.

## 2. METHODS

### 2.1. Image data

The first 400 images of natural scenes (images imk00001.iml to imk00400.iml) were downloaded from the natural stimuli collection of Hans van Hateren (<http://hlab.phys.rug.nl/archive.html>; accessed May 27, 2006) (van Hateren and van der Schaaf, 1998). Only those images that did not contain any man-made objects (buildings, streets, etc.) were included in the analysis. Furthermore, images of household and laboratory objects and images of plants or parts of plants were obtained with a 4-megabyte digital camera (Digital Ixus 400, Canon, Tokyo, Japan) in the botanical garden of the University of Jena and converted to grayscale images. Square details of maximal possible size were taken from the digital images by appropriate software (Photoshop, Adobe, Mountainview, CA). Examples of images are shown in Fig. 1.

Examples of monochrome (grayscale) graphic art were digitized by scanning reproductions from different art books. Care was taken that the reproductions scanned were of high quality and did not contain obvious artefacts (paper folds or cuts, stains, blotches, etc.). The esthetic quality of the images was well preserved in the reproductions, as judged on subjective grounds by one of the authors (C. R.), who is familiar with graphic art. The set of images originate from a wide variety of artists and different cultural backgrounds of the Western hemisphere. They include examples of different graphic techniques (etchings, engravings, lithographs, woodcuts, and other techniques), art from different centuries (15th century to 20th century) and art from different countries (Italy, Flanders, France, Germany, Spain, and other countries). Also, the images depict different subject matters (portraits, landscapes, buildings, animals and plants, persons, abstract art or others). Examples are shown in Fig. 2. Digitization was carried out with the help of two commercial scanners (Perfection 3200 Photo, Seiko Epson Corporation, Nagano, Japan; and ScanMaker 9600 XL, Microtek, Willich, Germany). No compression and image enhancement algorithms were applied. Non-square images were padded according to square ones prior to further processing. For padding, a uniform border was added with a grey value equal to the average grey value in the image. To assess whether the padding procedure introduced artefacts, square details of the largest possible sizes from all images of graphic art were also analyzed. Because results were very similar (Table 1), padded images were used for the rest of the analysis.

Scientific illustrations from different textbooks on genetics, anatomy or neuroscience were scanned and processed in exactly the same manner as graphic art. These illustrations included anatomical illustrations and maps, diagrams of neural connectivity and electrophysiological recordings, and schematic representations of histological features, metabolic pathways and molecules. All illustrations were produced by scientific illustrators and did not contain any photomicrographs of natural objects or scenes.

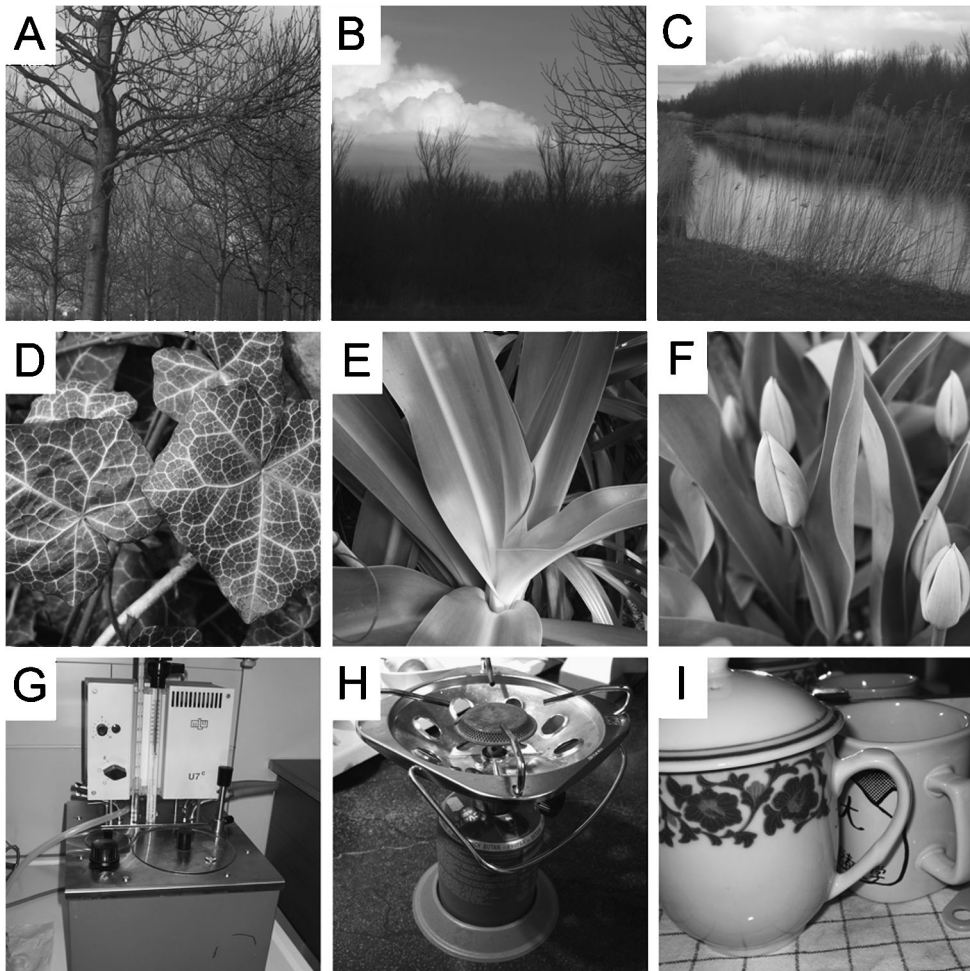


**Figure 1.** Examples of control images analyzed. (a)–(c). Natural scenes from the natural image collection of Hans van Hateren. (d)–(f) Close-up images of plants. (g)–(i) Images of a household and laboratory objects. Slope constants were  $-1.88$  (a),  $-2.15$  (b),  $-2.44$  (c),  $-2.57$  (d),  $-2.98$  (e),  $-3.49$  (f),  $-2.54$  (g),  $-2.68$  (h) and  $-3.16$  (i), respectively.

## 2.2. Image analysis

Image analysis was performed using Matlab. The test set consisted of gray value images of different dimensions. First, each input image was resized to  $1024 \times 1024$  pixels by bicubic interpolation. By default, for reducing the size of the image, a low-pass filter was applied before interpolation, to limit the impact of aliasing on the output image. The effect of the low pass filter is negligible in our analysis, since only a part of the frequency domain is analyzed that is not affected by the low-pass filter operation.

Next, each image was transformed into the frequency domain using Fast Fourier Transform. For each frequency, the rotational average of the power spectrum was

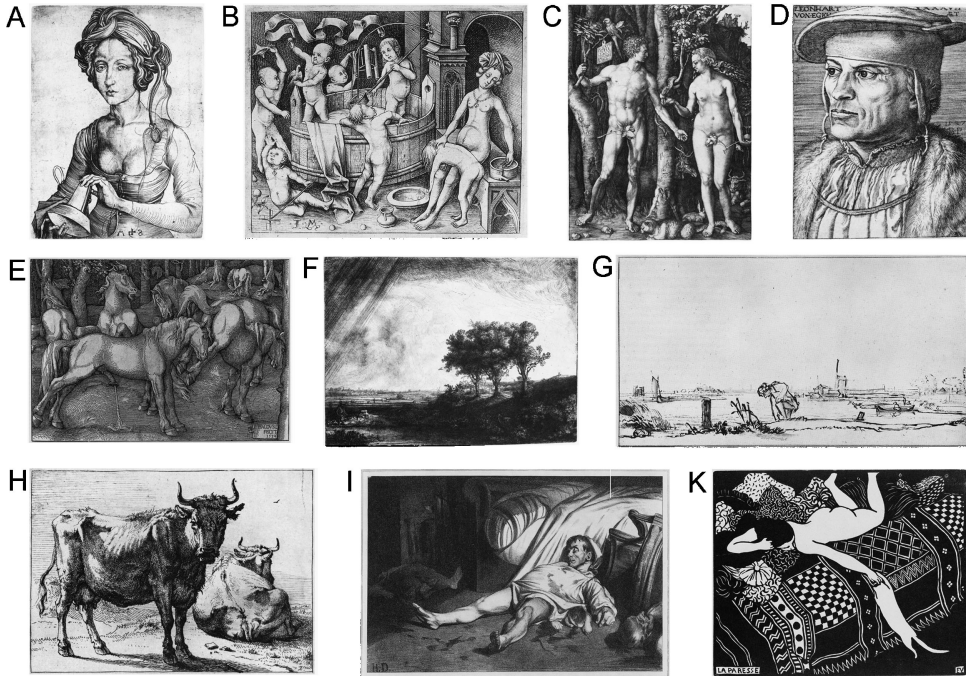


**Figure 2.** Examples of graphic art analyzed in the present study. (a) Engraving by Martin Schongauer, about 1470. (b) Engraving by Israel van Meckenem, about 1490. (c) Engraving by Albrecht Dürer, 1504. (d) Engraving by Barthel Beham, 1527. (e) Woodcut by Hans Baldung, 1534. (f) Etching by Rembrandt Harmensz van Rijn, 1643. (g) Drawing by Rembrandt Harmensz van Rijn, about 1650. (h) Etching by Paulus Potter. (i) Lithograph by Honoré Daumier, 1834. (k) Woodcut by Félix Vallotton, 1896. Slope constants were  $-2.14$  (a),  $-2.01$  (b),  $-2.60$  (c),  $-2.02$  (d),  $-1.95$  (e),  $-2.24$  (f),  $-1.91$  (g),  $-2.16$  (h),  $-2.42$  (i) and  $-1.95$  (k), respectively. Reproduced with permission from *Das Berliner Kupferstichkabinett*, Akademischer Verlag, Berlin, 1994 ((b) inventory number 976-1; (e), 916-2; (g), 5212; (i), 84-1912; (k) 167-1897; © Staatliche Museen zu Berlin, Kupferstichkabinett) and from *Meisterwerke alter Druckgraphik aus der Staatsgalerie Stuttgart*, Stuttgarter Galerieverein, Stuttgart, 1982/1983 ((a), (c), (d), (f), (h)); © Staatsgalerie Stuttgart, Graphische Sammlung).

computed. For further analysis, the log–log plane of frequency and power spectrum was used (Fig. 3a). The next step was a least squares fit of a line to the log–log power spectrum. To avoid artefacts in our analysis, for example due to low pass filtering, rectangular sampling, raster screen or noise in the images, only the frequency range between 10 and 256 cycles per image was used for interpolation (Fig. 3a). For fitting, data points were binned at regular intervals. For each image, the result is the slope of the line and the deviation of the data points from that line. The deviation was calculated as the sum of the squares of the deviations of the data points, divided by the number of data points. In total we analyzed five different data sets, consisting of natural scenes (208 images), graphic art (200), plants (206), objects (179) and illustrations (209).

**Table 1.**

Results for graphic art, calculated separately for distant and close-up views, and different cultural variables (techniques, centuries, countries of origin, and predominant subject matters). Means and standard deviations (SD) are given for the slope constants of the fitted line and for the deviations of the measured values from the fitted line.  $N$ : number of images analyzed in each category

	Slope (mean $\pm$ SD)	Deviation (mean $\pm$ SD)	$N$
All images, padded according to square images	$-2.10 \pm 0.32$	$0.012 \pm 0.014$	200
All images, largest possible square detail	$-2.07 \pm 0.37$	$0.015 \pm 0.018$	200
Distant views of complex scenes	$-1.95 \pm 0.24$	$0.008 \pm 0.008$	40
Close-up views	$-2.16 \pm 0.33$	$0.022 \pm 0.023$	40
Techniques			
Etching	$-2.07 \pm 0.23$	$0.014 \pm 0.016$	80
Engraving	$-2.07 \pm 0.23$	$0.005 \pm 0.006$	32
Lithograph	$-2.32 \pm 0.38$	$0.011 \pm 0.017$	20
Woodcut	$-2.11 \pm 0.36$	$0.014 \pm 0.014$	29
Other	$-2.07 \pm 0.45$	$0.013 \pm 0.013$	39
Century			
15th Century	$-2.01 \pm 0.19$	$0.007 \pm 0.008$	13
16th Century	$-2.02 \pm 0.26$	$0.006 \pm 0.009$	39
17th Century	$-2.08 \pm 0.21$	$0.015 \pm 0.014$	36
18th Century	$-2.05 \pm 0.24$	$0.015 \pm 0.016$	20
19th Century	$-1.87 \pm 0.33$	$0.015 \pm 0.012$	25
20th Century	$-2.28 \pm 0.36$	$0.013 \pm 0.017$	67
Country			
Italy	$-2.03 \pm 0.24$	$0.012 \pm 0.017$	48
Flanders	$-1.94 \pm 0.32$	$0.013 \pm 0.014$	34
France	$-2.16 \pm 0.26$	$0.008 \pm 0.007$	18
Germany	$-2.13 \pm 0.34$	$0.011 \pm 0.012$	63
Spain	$-2.30 \pm 0.36$	$0.014 \pm 0.019$	18
Other	$-2.22 \pm 0.32$	$0.015 \pm 0.015$	19
Subject matter			
Portrait	$-2.17 \pm 0.33$	$0.022 \pm 0.020$	38
Landscape	$-1.95 \pm 0.37$	$0.007 \pm 0.007$	17
Buildings	$-2.00 \pm 0.24$	$0.011 \pm 0.008$	20
Plants, animals	$-1.99 \pm 0.21$	$0.018 \pm 0.014$	11
People	$-2.08 \pm 0.26$	$0.008 \pm 0.009$	76
Abstract	$-2.43 \pm 0.45$	$0.010 \pm 0.009$	17
Other	$-2.06 \pm 0.30$	$0.015 \pm 0.024$	21

### 3. RESULTS

Figure 3a shows the relation between signal power and spectral frequency for the engraving depicted in Fig. 2a. Note that, for the frequency range analyzed (10 to 256 cycles per image), the individual binned data points deviate only slightly from the fitted straight line, which has a slope constant of close to  $-2$ . In the log-log plane, the slope of the fitted line represents the factor  $p$  (see Introduction).

In Fig. 3b, the results of slope constants  $\nu$ s deviations are given for each of the 200 examples of graphic art. The mean value for the slope constants is  $-2.1$ . For

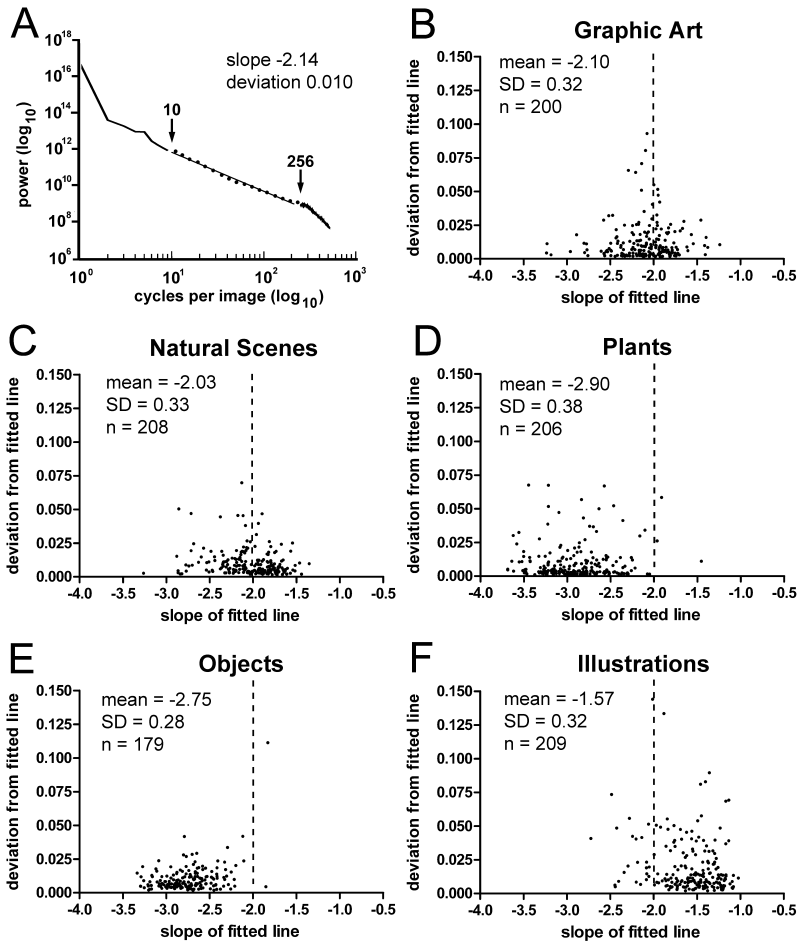


**Figure 3.** Results of the Fourier spectral analysis. (a) Fourier power is plotted as a function of frequency in the log–log plane. Values in the range of 10 to 256 cycles per image (arrows) were binned at regular logarithmic intervals (dots) and a straight line was fitted to the data points. The curve shows the values for the image displayed in Fig. 1a, b–f. Scatter diagrams showing the slopes of the fitted lines and the deviations of the measured data points from the fitted line for graphic art (b), natural scenes (c), plants (d), household and laboratory objects (e) and scientific illustrations (f).

60% of the images, the data points fitted a straight line as well as or better than the example shown in Fig. 3a (deviations equal or less than 0.01).

Figure 3 shows also the results of slope constants vs deviations for natural scenes (Fig. 3c), plants (Fig. 3d), household and laboratory objects (Fig. 3e), and scientific illustrations (Fig. 3f). Because not all these data sets displayed a Gaussian distribution, results were subjected to non-parametric statistical analysis (Kruskal–Wallis test with Dunn’s multiple comparison post-test). Slope constants and deviations for graphic art (Fig. 3b) and natural scenes (Fig. 3c) did not vary significantly from each other, as did results for plants and objects. The mean slope

constants for plants ( $-2.9$ ) and for objects ( $-2.8$ ) were significantly higher than those for graphic art and natural scenes ( $p < 0.001$ ) whereas the mean slope constant for illustrations ( $-1.6$ ) was significantly lower ( $p < 0.001$ ). Moreover, illustrations showed significantly higher deviations from the fitted line than the other image categories ( $p < 0.001$ ).

The images of plants and objects represent close-up views of one or a few objects. Under close-up viewing conditions, the fractal properties found in images of natural or complex scenes break down. The average slope values are higher because close-up images of objects usually contain a higher proportion of frequencies in the lower range than in the higher range. To assess whether, in our sample of graphic art, similar differences related to the viewing distance exist, we selected 40 images of close-up views (portraits, natures mortes, images of animals; for example, see Fig. 2a, d, h) and 40 images representing distant views of complex scenes (landscapes, etc.; for example, see Fig. 2b, g). Average slope values for the close-up views ( $-2.2$ ; Table 1) were significantly lower than those for the complex scenes ( $-2.0$ ; two-tailed Mann–Whitney test,  $p > 0.002$ ). Both values were similar to the average slope constant for the complete set of graphic art ( $-2.1$ ; Table 1).

We next asked whether the slope constants for graphic art depend on cultural variables, such as techniques, centuries and country of origin, and subject matters. Results in Table 1 show that differences for these variables were relatively small, if significant at all. Similar results were obtained for the deviations from the fitted lines (Table 1).

## 4. DISCUSSION

### 4.1. Similarities in image statistics between graphic art and natural scenes

Results from the present study show that examples of Western graphic art and natural scenes share statistical features in the Fourier domain. In both types of stimuli, the Fourier power falls close to linearity with spatial frequency when power is plotted against frequency in the log–log plane. The average slope constants for graphic art and natural scenes are near  $-2$  (Fig. 3b, c), indicating that Fourier power falls according to a power-law. Similar results were obtained previously for natural scenes by several researchers (Burton and Moorhead, 1987; Field, 1987; Ruderman and Bialek, 1994; Tolhurst *et al.*, 1992).

Our results also show that not all images of natural objects have slope values near  $-2$ . Plant images have significantly lower average slope constants (mean  $-2.9$ ; Fig. 3d) than natural scenes and graphic art. The lower slope constants reflect more frequencies in the lower range than in the higher range, when compared to graphic art and natural scenes, as would be expected for close-up views of single or a few objects. For example, the image of plants shown in Fig. 1d–f have slope values of  $-2.57$ ,  $-2.98$  and  $-3.49$ , respectively. Similarly, close-up views of household and laboratory objects (Fig. 1g–i) have slope values significantly smaller than  $-2.0$  (Fig. 3e).

Unlike images of plants and objects, images of scientific illustrations (Fig. 3f), which were scanned and processed in precisely the same way as the images of graphic art, have slope constants that are generally higher than  $-2$  (mean  $-1.6$ ). The vast majority of these images represent drawings composed predominantly of lines. This may explain the higher relative abundance of higher frequencies in the images and, hence, the higher slope constants.

Artifacts that may have influenced our results possibly include changes in gray scale calibration, noise and square sampling during reproduction and scanning of the images. However, it is unlikely that these artifacts have an effect on the results obtained. For natural scenes, the slope value of the lines in the log-log plane, which describes how Fourier power falls with frequency, is relatively robust to image manipulations, such as calibration in contrast or offset of gray value (for a review, see Ruderman, 1997). Moreover, the possible effect of artifacts due to noise, square sampling, and raster screens was minimized by the interpolation carried out to reduce image size to 1024 by 1024 pixels, and by restricting the scaling analysis to frequencies higher than 10 cycles/image and lower than 256 cycles/image (wavelength of 4 pixels). For this reason, it is unlikely that the results in the present study were biased, for example, by the reproduction of the works of art in art books. Likewise, artifacts induced by the scanning procedure (lack of scanner calibration) are not likely to affect significantly the range of frequencies analyzed in the present study. The scans thus represent suitable replacements of the original works of art in terms of their esthetic function, which is the focus of the present study.

#### 4.2. Scale invariance of graphic art

The  $1/f^2$  power spectrum implies that works of graphic art have fractal-like properties and display scale invariance, as previously shown for natural scenes (for reviews, see Olshausen and Field, 2000; Simoncelli and Olshausen, 2001). Fractal-like properties were reported previously for the abstract drip paintings by the 20th century artist Jackson Pollock (Taylor *et al.*, 1999). Confirming this study, the three works by this artist, which were included in the present study, had slope constants of 1.9, 2.1 and 2.3.

The relation between image statistics and visual system function may, however, be different for graphic art and natural scenes. It has been suggested that the visual system is adapted to the statistics in natural scenes by evolution, development and adaptation (David *et al.*, 2004; Field, 1987; Hoyer and Hyvärinen, 2002; Olshausen and Field, 1996; Parraga *et al.*, 2000; Sharpee *et al.*, 2006; Simoncelli, 2003; Simoncelli and Olshausen, 2001; Vinje and Gallant, 2000). The opposite seems to hold for esthetic stimuli. An artist creates a work of art by constant feedback with his own visual system, thereby adapting the work of art to features of his visual system (and not *vice versa*) (Zeki, 2002). This artistic adaptation is especially evident for graphic art, which shows close-up views, such as portraits or drawings of objects. While close-up photographs of objects generally display slope constants

lower than  $-2$  (Fig. 3d, e), artists seem to shift these slope constants in their works of art to higher average values (Table 1) so that, in the works of art, the ‘close-up’ views acquire Fourier statistics that resemble the fractal properties of natural (complex) scenes. This artistic paradox suggests that visual artists have implicit knowledge of the statistics of natural scenes; these statistics are, at least in part, reflected in the results of the Fourier analysis. Artists seem to apply this knowledge in their works of art, even when depicting views with non-fractal statistics. It has been shown that humans have a consistent esthetic preference across fractal images, regardless of the type of image (natural, man-made or computer-generated) (Hagerhall *et al.*, 2004; Spehar *et al.*, 2003).

Fractal-like image properties may be necessary, but they are not sufficient to induce esthetic perception for several reasons. First, examples of computer-generated images with fractal-like properties have been designed that may look natural but are not necessarily esthetically pleasing (Lee and Mumford, 1999; Olshausen and Field, 2000; Ruderman, 1997). Second, enough examples of plants, objects or illustrations can be found in the present image data set that have slope constants similar to those of examples of graphic art. Third, the esthetic appeal of art objects is generally considered more intense than that of natural scenes. Fourth, the Fourier spectra are computed by radially averaging the amplitudes of each frequency in the Fourier plot. By doing so, the information on the orientation of the frequencies in the image and their phase is lost in the analysis. Both features, however, can be expected to be important determinants of image structure and to contribute to esthetic appearance. Therefore, the sensory principles underlying esthetic perception remain to be elucidated. Nevertheless, the present results direct us to speculate that the biology of esthetic perception is linked to the coding of scale-invariant natural stimuli in the sensory systems. The coding of natural stimuli has been described as sparse and efficient (Hoyer and Hyvärinen, 2002; Lewicki, 2002; Olshausen and Field, 1996, 2004; Vinje and Gallant, 2000). A general and universal theory of esthetic perception based on the sensory coding of natural stimuli is presented in another article of this special issue (Redies, 2007). Finally, it should be noted that natural scenes and visual art differ in that art objects can evoke deeper esthetic feelings. This difference may relate to the fact that artists can adapt their works also to the intrinsic functional features of the nervous system (Redies, 2007).

In the present study, we demonstrated fractal-like image statistics for a subset of graphic art from the Western hemisphere. The universality of this finding in other forms of Western art and in art from other cultures remains to be established. The fractal structure of Jackson Pollock’s drip paintings (Taylor *et al.*, 1999) suggests that other forms of art may follow similar rules. Moreover, within the set of Western graphic art analyzed in the present study, the cultural variables listed in Table 1 do not have a prominent effect on the general image scaling properties. Based on these results, we speculate that scale invariance is a universal property of visual art. Exceptions may be some forms of contemporary art that are not intended to be esthetic, but follow other artistic rules. It would be interesting to find out

whether our hypothesis can be extended to esthetic perception in other senses that are optimally adapted to natural stimuli, for example, to music and the auditory system.

### Acknowledgements

The authors thank members of their research groups and the students of the ‘Sparse Coding’ seminar for discussions and suggestions, and Jens Geiling, Stefanie Deinhardt and Jan Hänisch for assistance with digitalization of images and computing. This work was presented as a poster at the Gordon Research Conference on ‘Sensory Coding and the Natural Environment’, held in Big Sky, Montana, August 27–September 1, 2006.

### REFERENCES

- Burton, G. J. and Moorhead, I. R. (1987). Color and spatial structure in natural scenes, *Appl. Phys.* **26**, 157–170.
- David, S. V., Vinje, W. E. and Gallant, J. L. (2004). Natural stimulus statistics alter the receptive field structure of V1 neurons, *J. Neurosci.* **24**, 6991–7006.
- Field, D. J. (1987). Relations between the statistics of natural images and the response properties of cortical cells, *J. Opt. Soc. Amer. A* **4**, 2379–2394.
- Hagerhall, C. M., Purcell, T. and Taylor, R. (2004). Fractal dimension of landscape silhouette outlines as a predictor of landscape preference, *J. Environ. Psychol.* **24**, 247–255.
- Hahnloser, R. H., Kozhevnikov, A. A. and Fee, M. S. (2002). An ultra-sparse code underlies the generation of neural sequences in a songbird, *Nature* **419**, 65–70.
- Hoyer, P. O. and Hyvärinen, A. (2002). Sparse coding of natural contours, *Neurocomputing* **44–46**, 459–466.
- Lee, A. B. and Mumford, D. (1999). An occlusion model generating scale-invariant images, in: *Proc. IEEE Workshop Statist. Comput. Theories Vision*, pp. 1–20. Fort Collins.
- Lewicki, M. S. (2002). Efficient coding of natural sounds, *Natur. Neurosci.* **5**, 356–363.
- Olshausen, B. A. and Field, D. J. (1996). Natural image statistics and efficient coding, *Network: Comp. Neuro. Syst.* **7**, 333–339.
- Olshausen, B. A. and Field, D. J. (2000). Vision and the coding of natural images, *Amer. Sci.* **88**, 238–245.
- Olshausen, B. A. and Field, D. J. (2004). Sparse coding of sensory inputs, *Curr. Opin. Neurobiol.* **14**, 481–487.
- Parraga, C. A., Troscianko, T. and Tolhurst, D. J. (2000). The human visual system is optimised for processing the spatial information in natural visual images, *Current Biol.* **10**, 35–38.
- Redies, C. (2007). A universal model of esthetic perception based on the sensory coding of natural stimuli, *Spatial Vision* **21**, 97–117.
- Ruderman, D. L. (1997). Origins of scaling in natural images, *Vision Research* **37**, 3385–3398.
- Ruderman, D. L. and Bialek, W. (1994). Statistics of natural images — scaling in the woods, *Phys. Rev. Lett.* **73**, 814–817.
- Sharpee, T. O., Sugihara, H., Kurgansky, A. V., Rebrik, S. P., Stryker, M. P. and Miller, K. D. (2006). Adaptive filtering enhances information transmission in visual cortex, *Nature* **439**, 936–942.
- Simoncelli, E. P. (2003). Vision and the statistics of the visual environment, *Curr. Opin. Neurobiol.* **13**, 144–149.

- Simoncelli, E. P. and Olshausen, B. A. (2001). Natural image statistics and neural representation, *Ann. Rev. Neurosci.* **24**, 1193–1216.
- Spehar, B., Clifford, C. W. G., Newell, B. R. and Taylor, R. P. (2003). Universal aesthetic of fractals, *Computers and Graphics* **27**, 813–820.
- Taylor, R. P., Micolich, A. P. and Jonas, D. (1999). Fractal analysis of Pollock's drip paintings, *Nature* **399**, 422.
- Tolhurst, D. J., Tadmor, Y. and Chao, T. (1992). Amplitude spectra of natural images, *Ophthalmic Physiol. Opt.* **12**, 229–232.
- van Hateren, J. H. and van der Schaaf, A. (1998). Independent component filters of natural images compared with simple cells in primary visual cortex, *Proc. Biol. Sci.* **265**, 359–366.
- Vinje, W. E. and Gallant, J. L. (2000). Sparse coding and decorrelation in primary visual cortex during natural vision, *Science* **287**, 1273–1276.
- Vinje, W. E. and Gallant, J. L. (2002). Natural stimulation of the nonclassical receptive field increases information transmission efficiency in V1, *J. Neurosci.* **22**, 2904–2915.
- Zeki, S. (1999). *Inner Vision*. Oxford University Press, Oxford, UK.
- Zeki, S. (2002). Vision and art: the biology of seeing, *Nature* **418**, 918–919.